Mother structures related to the hexagonal and cubic close packing in Cu$_{24}$ clusters: solvent-influenced derivatives

Eder Amayuelas,[a] Arkaitz Fidalgo-Marijuan,[a] Gotzone Barandika,[b,*] Begoña Bazán,[a,c] Miren-Karmele Urtiaga,[a] María Isabel Arriortua[a,c]

Compound **1** [Cu$_{24}$(*m*-BDC)$_{24}$(DMF)$_{20}$(H$_2$O)$_4$]·24DMF·40H$_2$O (*m*-BDC is 1,3-benzenedicarboxylate and DMF is *N,N*-dimethylformamide) has been synthesized and structurally characterized by X-ray diffraction. It consists of Cu$_{24}$-clusters arranged in such a way that 12 dimers are connected through *m*-BDC ligands. The clusters exhibit an internal cavity where crystallization molecules of DMF and water are located. Additionally, there are guest DMF and water molecules in the voids generated by the 3D packing of the Cu$_{24}$-clusters. The thermal stability of compound **1** has been also characterized, concluding that hydrogen bonds between solvent molecules are responsible for the robustness of the network. Compound **1** is similar to other seven compounds found in literature. This work is focused on the crystallochemical comparison of these compounds, which concludes that there are two mother structures related to the hexagonal and cubic close packing of polyhedra, respectively. Derivative compounds are produced by the presence of different solvent molecules (differences affecting both the nature and the number of the guest molecules).

INTRODUCTION

In supramolecular coordination architectures, metal−organic M$_{24}$-clusters (M=transition metal) have attracted particular interest due to their well-defined and confined cavities, high symmetry and stability, and rich chemical and physical properties and functions.[1-5] In the past decade, great advances have been done in the design, synthesis and characterization of these compounds, despite the difficulties they entail; for instance, the high requirements in crystallographic accuracy. Furthermore, crystal growth is especially relevant in this type of compounds since the principle of maximum space filling in crystal structures often produces outstanding phenomena like interpenetrated frameworks.[6-9] Therefore, the role of void-filling solvents is rather significant as different frameworks can be produced in dissolution-started crystallization processes. In fact, in these cases, solvents provide the Van der Waals forces driving the crystal growth, where those small molecules are strategically packed to stabilize the network. Solvent molecules can also complete coordination polyhedra around metal ions in SCFs (solid coordination frameworks). On the other hand, crystal growth has a direct influence on the morphology of the crystals.[10] Obviously, aspects related to the role of solvents are especially remarkable in porous compounds since, in many cases, the cavities contain solvent molecules.

This work is focused on a new SCF. This type of compounds has been extensively studied during the last decade thanks to the variety of structures that can be formed by using metal complexes as synthons.[11-15] In fact, this work reports on [Cu$_{24}$(*m*-BDC)$_{24}$(DMF)$_{20}$(H$_2$O)$_4$]·24DMF·40H$_2$O (**1**), where *m*-BDC is 1,3-benzenedicarboxylate (Scheme 1), and DMF is *N,N*-dimethylformamide, since the features exhibited by this compound gives us the opportunity of discussing about most of the above mentioned aspects. Thus, compound **1** consists of Cu$_{24}$-clusters arranged in such a way that 12 dimers are connected through *m*-BDC ligands.
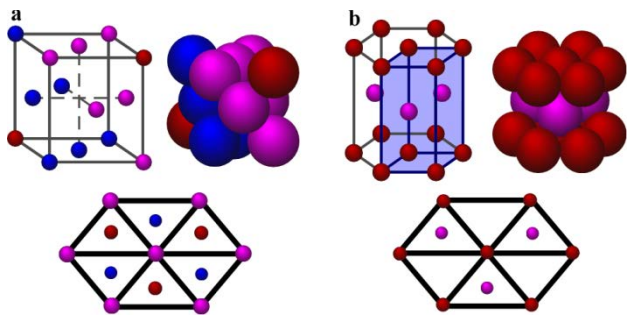

1,3-benzenedicarboxylate

Scheme 1. Lewis Structure of 1,3-benzenedicarboxylate (*m*-BDC).

Interest of compound **1** lies on the fact that seven similar clusters have been reported so far.[16-18] However, comparison of the eight compounds (including compound **1**) reveals the variety in the 3D packing fashions produced by similar, discrete, large clusters. This comparison also permits discussion on the role of solvents acting as crystallization molecules, and their influence on the packing modes. Furthermore, this work provides some examples of the risk associated to visualization of crystal structures, especially when figures intend to transmit the existence of large cavities by omitting the presence of crystallization molecules.

Another point for discussion is the risk associated to the interpretation of raw crystallographic data. Thus, while structural parameters for the eight compounds to be compared are quite different, a deep analysis reveals that they form two families: related to the hexagonal and cubic close packing of spheres (HCP and CCP, respectively, Scheme 2). Finally, as compound **1** has been synthesized through two distinct routes, this work also presents an example of the role of crystallization helpers yielding crystals with different sizes.[19]

Scheme 2. (a) Cell for cubic close packing. (b) Cell for hexagonal close packing.

Experimental section

General

All solvents and chemicals were used as received from reliable commercial sources. The reagents protoporphyrin IX, 1,3-isophthalic acid, copper(II) nitrate hydrate 99% and the solvent *N,N*-dimethylformamide (DMF, 99.8%) were purchased from Sigma-Aldrich Co.

Synthesis of $[Cu_{24}(m\text{-}BDC)_{24}(DMF)_{20}(H_2O)_4]\cdot24DMF\cdot40H_2O$

Cu(NO2)3·xH2O (12.9 mg, 0.06 mmol) and 1,3-isophthalic acid (m-BDC) (9.9 mg, 0.06 mmol) were added to DMF (4.5 mL) in a small capped vial and heated to 100 °C for 72 h, yielding diffraction quality prismatic turquoise crystals. Adding (5.9 mg, 0.01 mmol) of protoporphyrin IX to the above mentioned procedure, higher quality and bigger crystals were obtained. (Found: C, 38.13(4); H, 3.78(5); N, 2.38(3); O, 32.65(3). Calc. for: C237H232Cu24N16O133; C, 40.92; H, 3.36; N, 3.22; O, 30.58).

Single-crystal X-ray diffraction

Prismatic turquoise single-crystals of compound **1** with dimensions given in Table 1 were selected under polarizing microscope and mounted on MicroMounts™. Single-crystal X-ray diffraction data were collected at 100 K- on a SuperNova single source diffractometer with Cu Kα radiation (λ = 1.54184 Å). Data frames were processed (unit cell determination, intensity data integration, correction for Lorentz and polarization effects,[20] and analytical absorption correction) using the CrysAlisPro software package.[21]

The structure of **1** was solved in the triclinic *P*-1 space group with Superflip program,[22] which allowed us to obtain the position of Cu atoms, as well as some of the oxygen, nitrogen and carbon atoms of the isophthalic acid and DMF molecules. The initial refinement of the crystal structure was performed by conjugate-gradient least-squares using the CGLS instruction using SHELXL-97 program,[23] since the final cycles were performed by full matrix least-squares based on F^2, using SHELXH-97 program[23] in OLEX[24] obtaining the remaining nitrogen, oxygen and carbon atoms. Anisotropic thermal parameters were used for all nonhydrogen atoms involved in the cuboctahedric, as well as for DMF molecules fully occupying the crystallographic positions. The water and DMF solvent molecules partially occupying the crystallographic positions as well as the hydrogen atoms were refined isotropically (Figure S1, Suplementary Information†). The hydrogen atoms of the DMF and water molecules were not considered due to the lack of density in the residual density map; however they are included in the formula. Although 36 DMF and 24 water molecules positions were localized during the crystal structure refinement process, many of the solvent molecules were disordered in the crystal and the resulting electron density was found to be non interpretable (density corresponding to 520 e⁻ was removed per unit cell). Taking into account the single crystal experimental density[25] (1.346(5) g·cm⁻³), the removed electrons and the calculated free effective volume (explained below), our estimation is that 8 DMF and 20 water molecules per formula unit have been ignored during the structure refinement process, although they were included in the chemical formula. The solvent contribution to the structure factors was taken into account by back-Fourier transformation of all density found in the disordered area using the SQUEEZE program in PLATON.[26] The diffraction data was able to show DMF solvent molecules in 16 different positions giving a total occupancy of 12 molecules. In the case of water molecules, 20 H_2O were disordered in 23 different positions. The total of 20 coordination DMF molecules gives a total occupancy of 16, since two of the four coordination water positions were fully occupied and other two were disordered in four positions with 50 % each.

The position of some carbon, nitrogen and oxygen atoms in the DMF molecules were fixed using DFIX and DANG instructions in the refinement to adjust the C-N distance to 1.45 or 1.33 Å, the C=O distance to 1.23 Å and the C–N–C angle to 120°. Bond distances and angles, atomic coordinates, anisotropic thermal parameters and hydrogen atom coordinates are given in Tables S2-S4, Suplementary Information†.

From a crystallographic point, compound **1** can be described by using Z=2, in accordance with the space group and the asymmetric unit. However, Z'=1 has been considered because this way the whole cuboctahedric is represented in the chemical formula.

Table 1. Crystallographic data for **1**.

Compound	[Cu$_{24}$(*m*-BDC)$_{24}$(DMF)$_{20}$(H$_2$O)$_4$]·24DMF·40H$_2$O
Formula	C$_{297.58}$H$_{466}$Cu$_{24}$N$_{35.6}$O$_{172.7}$
FW, g·mol^{-1}	8830.49
Crystal system	Triclinic
Space group (no. 2)	$P\bar{1}$
a, Å	24.4797(3)
b, Å	24.5938(3)
c, Å	25.2374(3)
α, deg	118.4357(13)
β, deg	111.9694(11)
γ, deg	94.2287(10)
V, Å^3	11784.9 (2)
Z	1
ρ_{obs}, ρ_{cal}, g·cm^{-3}	1.346(5), 1.072
F(000)	3784
μ, mm^{-1}	1.737
Crystal size, mm	0.27 x 0.21 x 0.08
Absorption correction	Analytical
Radiation, λ, Å	1.54184
Temperature, K	100(2)
Reflections collected, unique	155317, 41318 (R_{int}=0.04)
Limiting indices	-29<=*h*<=29 -27<=*k*<=28 -30<=*l*<=28
Refinement method	Conjugate-gradient and full-matrix least-squares on F^2
Final *R* indices [I > 2σ(I)]^a	R1 = 0.0859, wR2 = 0.2564
R indices (all data)^a	R1 =0.0975, wR2 = 0.2744
Goodness of fit on F^2	1.087
Parameters /restraints	2154 / 47

^{a}R1=[(|F$_0$|- |F$_c$|)]/|F$_0$|. wR2=[[w|F$_0$|^2-|F$_c$|^2)^2]/[*w*(|F$_0$|^2)^2]$^{1/2}$

Physicochemical characterization techniques

The IR spectra were collected on a JASCO FT/IR-6100 spectrometer at room temperature at the range of 4000-400 cm^{-1}, in KBr pellets (1% of the sample). C, H, N and O elemental analyses were measured using a Euro EA 3000 elemental analyzer. Thermogravimetric analyses were carried out using a NETZSCH STA 449F3 thermobalance. A crucible containing approximately 10 mg of sample was heated at 5 °C min^{-1} in the temperature range 30-600 °C. The thermal behaviour was also studied using X-ray thermodiffractometry. A Bruker D8 Advance Vantec diffractometer (Cu-Kα radiation) equipped with a variable-temperature stage (Anton Paar HTK2000) with a Pt

sample holder was used in the experiments. The powder patterns were recorded in 2θ steps of 0.0333° in the 5-38° range, counting for 0.8 s per step and increasing the temperature at 15 °C·min^{-1} from room temperature to 600 °C.

Results and Discussion

Crystal Growth

As commonly experienced by researches, sometimes the result of a synthetic route is not desired one, and this is exactly what happened in the synthesis of compound **1**. In fact, we intended to produce metalloporphyrin-based SCFs,[27-30] but instead the synthesis yielded large, good-quality crystals of **1**. Then, we confirmed that the presence of protoporphyrin IX was not necessary to synthesize compound **1**. However, synthesis of **1** without protoporphyrin IX results in smaller, lower-quality, single crystals. Therefore, protoporphyrin IX acts as a crystallization helper. Figure 1 shows the aspect of the single crystals obtained with and without the crystallization helper. As observed, in both cases single crystals exhibit a prismatic habit. However, the use of the helper results in crystals up to ten times larger.
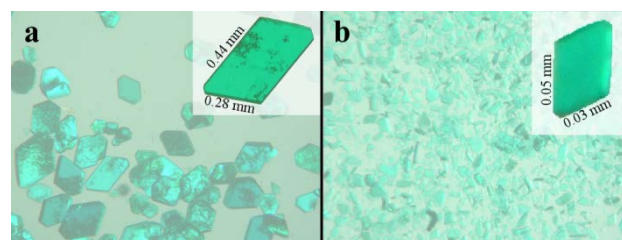

Fig. 1 Single crystals of compound **1** using the protoporphyrin IX as a crystallization helper (a), and without it (b).

Crystal Structure

Compound **1** consists of Cu$_{24}$-clusters arranged in such a way that 12 dimers are connected through *m*-BDC ligands (Figure 2). The *m*-BDC ligands are also responsible for the connections between the Cu^{II} ions forming the dimers. The clusters exhibit an internal cavity where crystallization molecules of DMF and water are located. Additionally, there are guest DMF and water molecules located in the voids generated by the 3D packing of the Cu$_{24}$-clusters (this point will be discussed below).
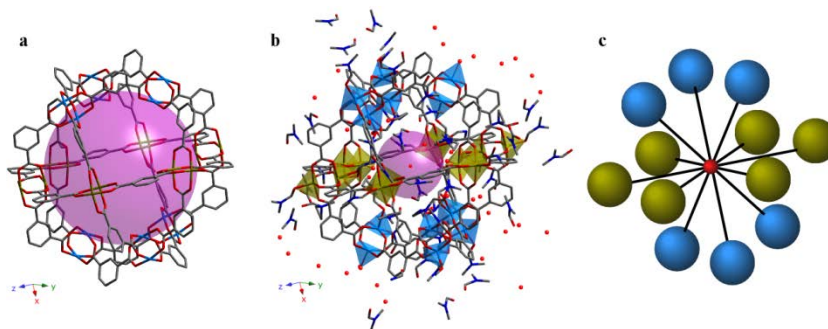

Fig. 2 View of the Cu$_{24}$-cluster (a) where solvent molecules have been omitted, and (b) where localized solvent molecules per formula unit are shown. The purple spheres represent the accessible volume: (a)=2145 Å^3, (b)=904 Å^3. Other color codes: C, grey; O, red; Cu (central), green; and Cu (upper and lower), blue. Hydrogen atoms are omitted for clarity. (c) Schematic view of the Cu$_{24}$-cluster where blue and green spheres account for the twelve dimmers per cluster.

The space group is *P*-1 implying that there is an inversion centre. As observed in Figure 2, the Cu_{24}-clusters are cuboctahedric units, and the twelve dimers consist of two Cu^{II} square pyramids (SP). The disposition of the twelve dimers is analogous to the cubic close packing of spheres (CCP), but in this case the central position is occupied by a crystallization molecule of water (located at an inversion centre).

Each SP has four oxygen atoms belonging to four different *m*-BDC ligands. Both SPs in each dimer are linked through Cu-O-C-O-Cu bridges, so they have their bases opposite to each other. The apical positions are occupied by DMF and water molecules: eight dimers have DMF molecules on both apical positions (16 DMF) and four dimers have 1:1 DMF:water (4 DMF and 4 water) (Table 2). This is, there are 20 coordinated DMF molecules per cluster, and 4 water molecules. Taking the centre of the cluster as a reference, the dimers are located in a radial fashion; one of the apical ligands points to the internal cavity while the other points to the exterior.

Table 2 DMF and water molecules coordinated to Cu^{II} dimmers.

	DMF	DMF : H_2O (1:1)	H_2O
Number of Cu^{II} dimers	8	4	--
Number of molecules	16	4:4	--

According to the chemical formula, and including the removed $520 e^-$ with the SQUEEZE program (as explained in the "Single-crystal X-ray diffraction" section), 24 DMF and 40 water molecules have been identified as crystallization molecules. As mentioned before, one of those internal water molecules is localized at the centre of the cluster, being the reference point around which the CCP disposition of the dimers produces the cluster.

The average diameters of the cluster are 32 Å (including terminal ligands) and 24 Å (excluding terminal ligands). Calculation of the diameter of the internal cavity omitting the guest molecules produces a value of 16 Å (volume of 2145 $Å^3$). Nevertheless, as observed in Figure 2, if considering internal guest molecules, this cavity is quite smaller (904 $Å^3$). In fact, the real value is slightly lower because, even if most of the ignored solvent molecules during structure refinement process are located outside the internal cavities, some of them do correspond to the internal cavity.

The clusters are 3D packed as shown in Figure 3. As observed, the central planes of the clusters (in green) are packed along the [100] direction. The intercluster connections take place through hydrogen bonds between the coordinated DMF and H_2O molecules in the dimers and the guest molecules. Most extended analysis of supramolecular structure will be done in the section devoted to comparison of **1** to the rest of similar clusters.
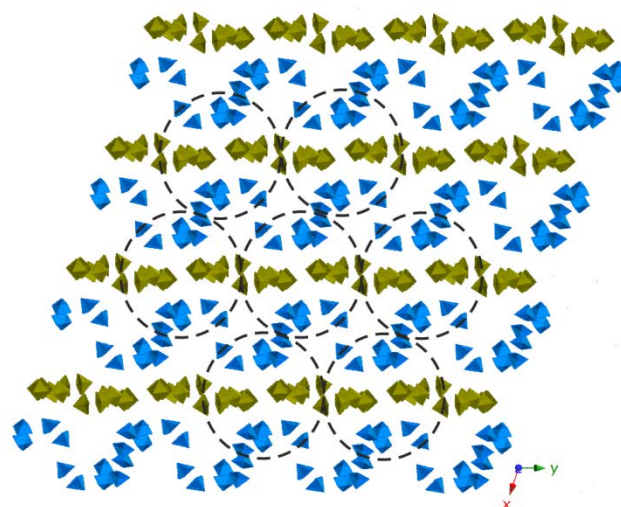

Fig. 3 [001] view of the supramolecular 3D framework for compound **1**. Each dotted circle marks a cluster. Green and blue polyhedra are the twelve dimmers per Cu_{24}-cluster. Solvent molecules and hydrogen atoms are omitted for clarity.

Infrared Spectroscopy

IR data show characteristic bands for *m*-BDC ligands of compound **1** (Figure 4). The bands at about 3402 cm^{-1} and 765-700 cm^{-1} were assigned to the C–H bond of the benzene rings. The bands at 2930 cm^{-1} and 1680 cm^{-1} were assigned to the O–H and C=O bonds of the carboxylic groups, respectively. Finally, the bands at 1630–1441 cm^{-1} were assigned to C=C stretching mode vibration.
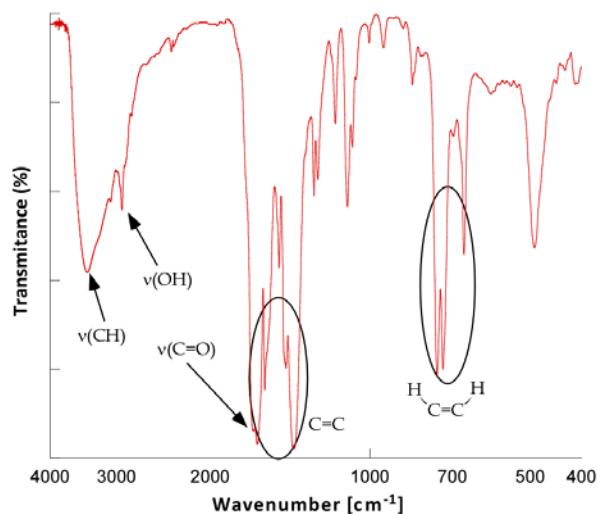

Fig. 4 Infrared spectra for compound **1**.

Thermogravimetry

The thermogravimetric decomposition curve for compound **1** shows a two-stage mass loss (Figure 5). The first step occurs between 20–230 ^0C with 27.2% weight loss. This value has been attributed to crystallization and coordination molecules of water

and DMF (25.9%). The second step is an overlapped process that occurs between 230-310 °C with 47.8% weight loss relative to the organic ligands of the cuboctahedron (41.8%) and coordinated DMF and water molecules (12.11%). The residue has been identified by X-ray powder diffraction as CuO [S.G. C2/c, a=4,6850 Å; b=3,4230 Å; c=5,1320 Å; β=99,52 °].[31]
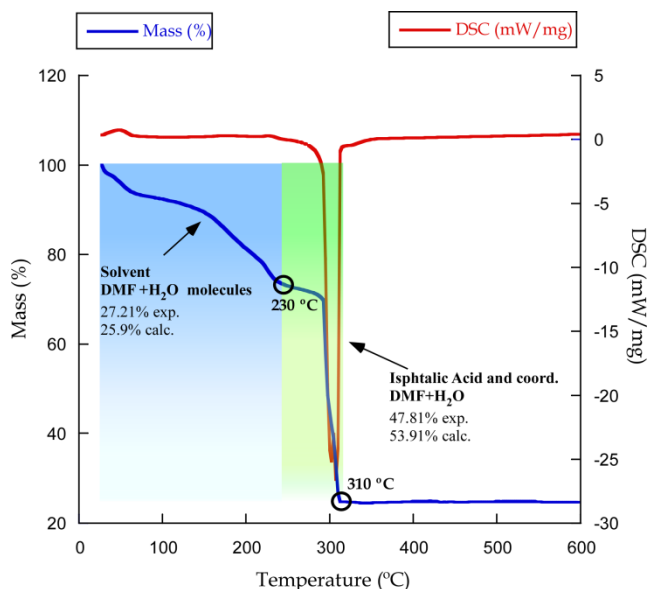

Fig. 5 Termogravimetric analysis for compound **1**.

X-ray thermodiffractometry

The thermal behaviour of compound **1** was also studied by X-ray thermodiffractometry (Figure S2, Suplementary Information†). Compound **1** keeps crystallinity until 165 ºC. At higher temperatures, the removal DMF and H_2O solvent molecules provokes the formation of an amorphous phase, forming CuO from 280 ºC.

Comparison of similar Cu_{24} clusters

A search in the CSD[32] (Cambridge Structural Database) shows 594 structures with pentacoordinated copper dimers similar to the one exhibited by compound **1**. However, just 7 of them are cuboctahedral $Cu_{24}(m$-BDC)-clusters. Therefore, the crystal structures of these compounds have been analyzed. Their chemical formula are: $[Cu_{24}(m$-BDC$)_{24}$ (MeOH$)_{24}]\cdot xS$[18] (hexagonal) (**2**), a-MOP-1[16] $[Cu_{24}(m$-BDC$)_{24}$(DMF$)_{14}$(H$_2$O$)_{10}]\cdot 50H_2O\cdot 6DMF\cdot 6C_2H_5OH$ (**3**), $[Cu_{24}(m$-BDC$)_{24}$(S$)_{24}]\cdot xS$[17] (**4**), $[Cu_{24}(m$-BDC$)_{24}$(Py$)_{12}$(MeOH$)_{12}]\cdot xS$[18] (**5**), c-MOP-1[16] $[Cu_{24}(m$-BDC$)_{24}$(H$_2$O$)_{24}]\cdot 42H_2O$ (**6**), $[Cu_{24}(m$-BDC$)_{24}$(MeOH$)_{24}]\cdot xS$[18] (cubic) (**7**) and $[Cu_{24}(m$-BDC$)_{24}$(MeOH$)_{24}]\cdot xS$[18] (monoclinic) (**8**). Therefore, similar arrangement is produced with other solvents distinct than DMF and water that act both as coordinated ligands and as crystallization molecules. In addition, the number of solvent molecules acting as crystallization molecules is variable.

Table S1 in the Suplementary Information† summarizes the most significant crystallographic parameters for those compounds. As previously said, these 7 compounds have been selected because they exhibit similar Cu_{24}-clusters. However, their different packing fashions are reflected in the distinct cell parameters, and they are related to the variety of solvent molecules.

As previously said, even if have provided the best of the possible structure refinement, we have not been able to localize all the crystallization molecules. In fact, comparison of the R indices for the rest of similar compounds (Table S1, Suplementary Information†) indicates that in most of the cases structural refinement has been carried out by omitting the solvent molecules. However, those solvent molecules are responsible for the stabilization of the crystal structure. In fact, removing of DMF and H_2O molecules produce the collapse of the crystal structure as shown by thermogravimetric and thermodiffraction analysis (Figures 5 and S2, Suplementary Information†).

If we analyze the packing of compound **1** (Figure 3), we can observe the layered nature of the 3D framework. Thus, as previously mentioned, the central planes of the cluster (green) are packed along the [100] direction. This way, the dimers above and below these planes (blue) are localized in between. As observed in Figure 6, layered frameworks can also be observed for compounds **2-5**.
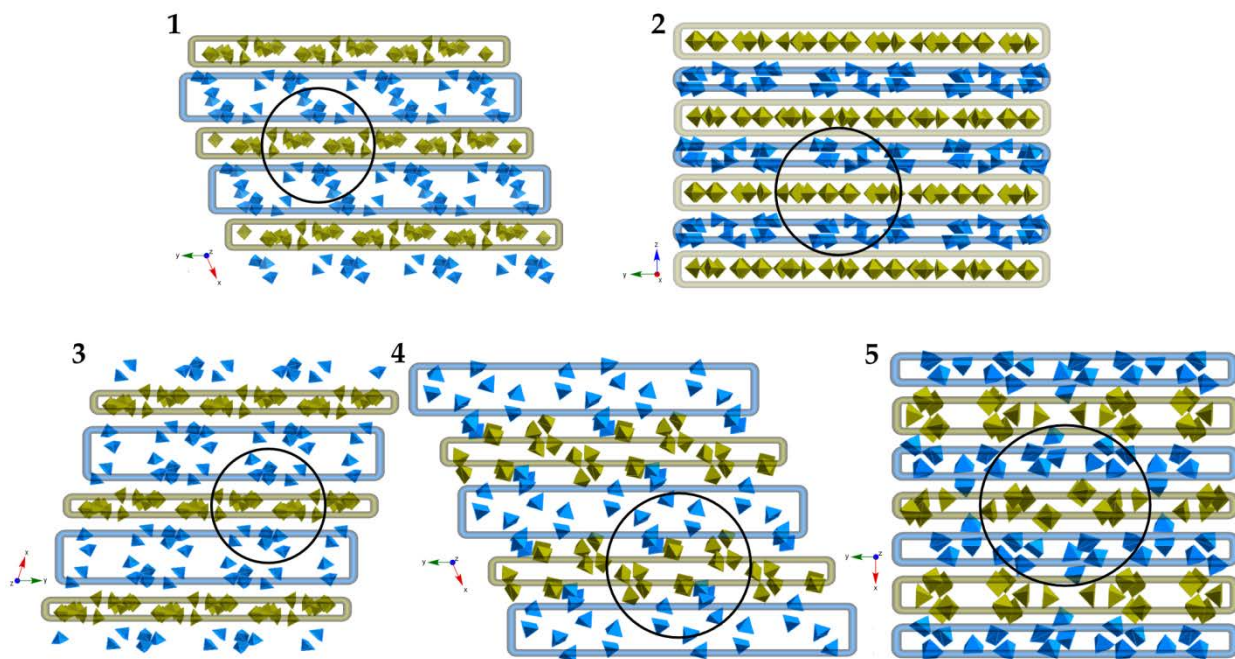
Fig. 6 Layered 3D frameworks for compounds **1-5**. Dotted circles mark the Cu_{24}-clusters. Green and blue plyhedra are the twelve dimmers per Cu_{24}-cluster.

It is worth noticing that compounds **3-5** are triclinic, and the clusters also exhibit the CCP fashion observed for **1**. However, cluster of compound **2** is of the HCP-type. Thus, this allows the unit cell to conserve the hexagonal symmetry (space group for **2** is $P6_3/m$).

Compounds **6-8** also exhibit a CCP-type cluster but they merit special attention. As observed in Table S1 (Suplementary Information†), structural parameters for cubic compounds **6** and **7** (space group is Im-3m) indicate that they have the same skeleton, so they will be described together. Thus, as a result of the cubic space group, the 3D framework for compound **6** (and **7**) is a layered structure (Figure 7) where planes contain both types of dimers (blue and green ones). On the other hand, compound **8** adopts an intermediate packing fashion between the high symmetrical compound **6** (and **7**) and the low symmetrical, triclinic compounds **1**, **3**, **4**, and **5**. In fact, two interpenetrated layered frameworks are observed for **8** (Figure 7) where clusters are packed in perpendicular planes.
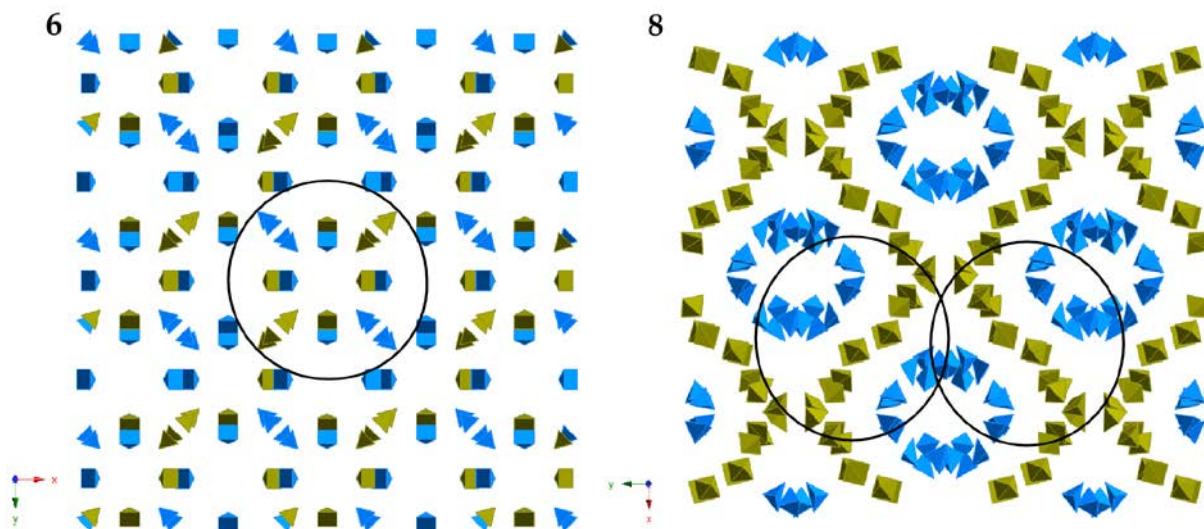

X

Fig.7 3D framework for compounds **6** (or **7**) and **8**. Dotted circles mark the Cu_{24}-clusters. Green and blue polyhedra are the twelve dimmers per Cu_{24}-cluster. Clusters for **8** are packed in two different orientations.

Therefore, the presence of MeOH in compounds **2** and **6** as a solvent gives rise to the highest symmetry, also producing both possible alternatives: hexagonal and cubic. These ideal packing fashions can be observed in figure 8 where a different view of the

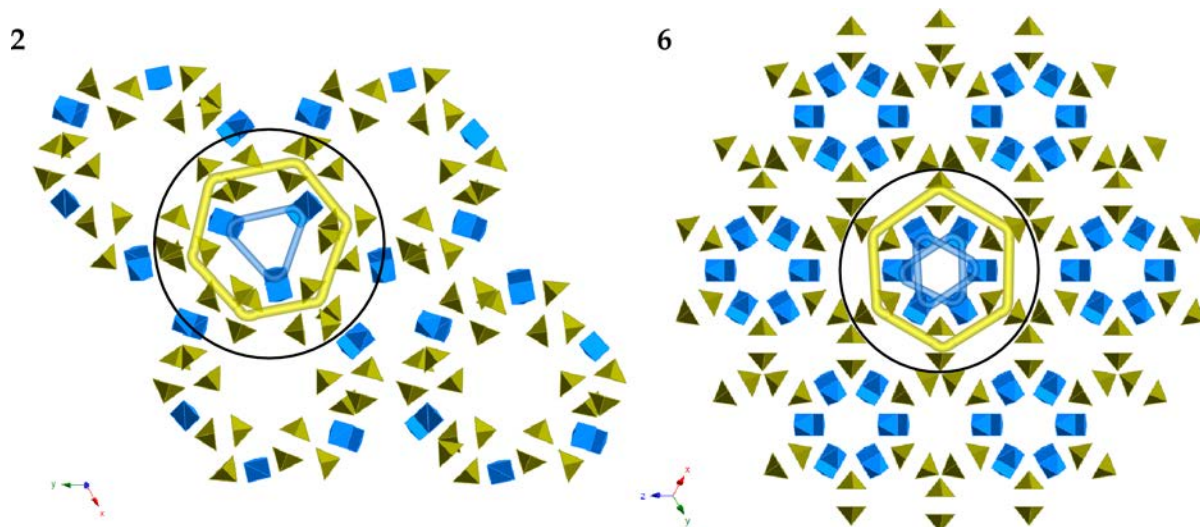3D frameworks for compounds **2** (hexagonal) and **6** (cubic) is shown.

Fig. 8 Mother structures for Cu$_{24}$-clusters: HCP-type (compound **2**) and CCP-type (compounds **6** and **7**).

As said before, we have made a special effort in locating the maximum number of molecules of solvent in the structural refinement of compound **1**. As a consequence, we have located a molecule of water right in the centre of the cluster. Therefore, those central water molecules seem to be the reference for the clusters to be formed and for the packing to be extended along the three directions of the space. On the other hand, the fact that both possible clusters (cubic and hexagonal) are related to the close packing of spheres makes us think of the similarities between these 3D arrays and the simple metal frameworks. At this point of the discussion, it is worth noticing that small molecules acting as coordinated ligands and as crystallization molecules are able to accumulate quite a high number of metal ions producing a variety of solids that are similar but not equal. So, we wonder if geological accumulation of metal deposits might have something to do with the formation of clusters like compounds **1-8**.

Conclusions

Comparison of compound **1** with similar ones found in literature reveals the existence of two mother structures related to the hexagonal and cubic close packing of polyhedra, respectively. Derivatives of these mother compounds depend on the solvents used in syntheses. Solvent molecules act both as ligands and as crystallization guest molecules. The variety in 3D frameworks observed for the eight compared compounds is attributable to the fact that solvents of different nature can play the same roles. Thus, not only the nature but also the number of solvent molecules is variable for the analyzed compounds, accounting for the flexibility of these host networks to accommodate different guests.

Acknowledgements

Notes and references

[a] *Departamento de Mineralogía y Petrología, Universidad del País Vasco (UPV/EHU), Barrio Sarriena s/n, 48940 Leioa, Bizkaia*
[b] *Departamento de Química Inorgánica Universidad del País Vasco (UPV/EHU), Barrio Sarriena s/n, 48940 Leioa, Bizkaia.*
[c] *BCMaterials, Basque Center for Materials, Applications and Nanostructures, Parque Tecnológico de Zamudio, Ibaizabal Bidea, Edificio 500-Planta 1, 48160 Derio, Bizkaia.*

1. H. Furukawa, J. Kim, N. W. Ockwig, M. O'Keeffe and O. M. Yaghi, *J. Am. Chem. Soc.*, 2008, **130**, 11650-11661.
2. Y. Ke, D. J. Collins and H.-C. Zhou, *Inorg. Chem.*, 2005, **44**, 4154-4156.
3. G. J. McManus, Z. Wang and M. J. Zaworotko, *Cryst. Growth Des.*, 2004, **4**, 11-13.
4. T.-F. Liu, Y.-P. Chen, A. A. Yakovenko and H.-C. Zhou, *J. Am. Chem. Soc.*, 2012, **134**, 17358-17361.
5. M. Tonigold, J. Hitzbleck, S. Bahnmueller, G. Langstein and D. Volkmer, *Dalton Trans.*, 2009, 1363-1371.
6. X. Li, R. Cao, D. Sun, W. Bi, Y. Wang, X. Li and M. Hong, *Cryst. Growth Des.*, 2004, **4**, 775-780.
7. L. Han, Y. Zhou, W.-N. Zhao, X. Li and Y.-X. Liang, *Cryst. Growth Des.*, 2009, **9**, 660-662.
8. R. Mondal, T. Basu, D. Sadhukhan, T. Chattopadhyay and M. k. Bhunia, *Cryst. Growth Des.*, 2009, **9**, 1095-1105.
9. B. Moulton and M. J. Zaworotko, *Chem. Rev.*, 2001, **101**, 1629-1658.
10. S. O. Ferreira and Editor, *Advanced Topics on Crystal Growth*, 2013.
11. H. Furukawa, K. E. Cordova, M. O'Keeffe and O. M. Yaghi, *Science*, 2013, **341**, 974.
12. M. O'Keeffe and O. M. Yaghi, *Chem. Rev.*, 2012, **112**, 675-702.
13. M. Li, D. Li, M. O'Keeffe and O. M. Yaghi, *Chem. Rev.*, 2014, **114**, 1343-1370.
14. T. R. Cook, Y.-R. Zheng and P. J. Stang, *Chem. Rev.*, 2013, **113**, 734-777.

15. F. Gandara, H. Furukawa, S. Lee and M. Yaghi Omar, *J. Am. Chem. Soc.*, 2014, **136**, 5271-5274.
16. M. Eddaoudi, J. Kim, J. B. Wachter, H. K. Chae, M. O'Keeffe and O. M. Yaghi, *J. Am. Chem. Soc.*, 2001, **123**, 4368-4369.
17. J.-R. Li and H.-C. Zhou, *Nat. Chem.*, 2010, **2**, 893-898.
18. B. Moulton, J. Lu, A. Mondal and M. J. Zaworotko, *Chem. Commun.*, 2001, 863-864.
19. I. Bruzaite, V. Snitka, V. Mizariene, L. Limanauskas and V. Lendraitis, *Int. J. Nanomanuf.*, 2010, **5**, 205-213.
20. W. Yinghua, *J. Appl. Crystallogr.*, 1987, **20**, 258-259.
21. , Agilent Technologies UK Ltd.: Oxford, U. K., 2012.
22. L. Palatinus and G. Chapuis, *J. Appl. Crystallogr.*, 2007, **40**, 786-790.
23. G. M. Sheldrick, *Acta Crystallogr., Sect. A Found. Crystallogr.*, 2008, **A64**, 112-122.
24. O. V. Dolomanov, L. J. Bourhis, R. J. Gildea, J. A. K. Howard and H. Puschmann, *J. Appl. Crystallogr.*, 2009, **42**, 339-341.
25. P. Roman and J. M. Gutierrez-Zorrilla, *J. Chem. Educ.*, 1985, **62**, 167-168.
26. A. L. Spek, *Acta Crystallogr., Sect. C Struct. Chem.*, 2015, **71**, 9-18.
27. A. Fidalgo-Marijuan, G. Barandika, B. Bazan, M. K. Urtiaga and M. I. Arriortua, *Polyhedron*, 2011, **30**, 2711-2716.
28. A. Fidalgo-Marijuan, G. Barandika, B. Bazan, M. K. Urtiaga and M. I. Arriortua, *Crystengcomm*, 2013, **15**, 4181-4188.
29. A. Fidalgo-Marijuan, G. Barandika, B. Bazan, M. K. Urtiaga, L. Lezama and M. I. Arriortua, *Inorg. Chem.*, 2013, **52**, 8074-8081.
30. A. Fidalgo-Marijuan, G. Barandika, B. Bazan, M. K. Urtiaga, E. S. Larrea, M. Iglesias, L. Lezama and M. I. Arriortua, *Dalton Trans.*, 2015, **44**, 213-222.
31. S. Asbrink and L. J. Norrby, *Acta Crystallogr., Sect. B*, 1970, **26**, 8-15.
32. F. H. Allen, *Acta Crystallogr., Sect. B Struct. Sci.*, 2002, **B58**, 380-388.